J Neurophysiol 101: 958–968, 2009.
First published December 10, 2008; doi:10.1152/jn.90547.2008.

Gain Modulation of Neuronal Responses by Subtractive and Divisive Mechanisms of Inhibition

Asli Ayaz and Frances S. Chance
Department of Neurobiology and Behavior, University of California, Irvine, California

Submitted 9 May 2008; accepted in final form 4 December 2008

Ayaz A, Chance FS. Gain modulation of neuronal responses by subtractive and divisive mechanisms of inhibition. *J Neurophysiol* 101: 958–968, 2009. First published December 10, 2008; doi:10.1152/jn.90547.2008. Gain modulation of neuronal responses is widely observed in the cerebral cortex of both anesthetized and behaving animals. Does this multiplicative effect on neuronal tuning curves require underlying multiplicative mechanisms of integration? We compare the effects of a divisive mechanism of inhibition (noisy excitatory and inhibitory synaptic inputs) with the effects of two subtractive mechanisms (shunting conductance and hyperpolarizing current) on the tuning curves of a model cortical neuron. We find that, although the effects of subtractive inhibition can appear nonlinear, they are accompanied by a change in response threshold and are best described as a vertical shift along the response axis. Increasing noisy synaptic activity divisively scales the model responses, reproducing a response-gain control effect. When mutual inhibition between subpopulations of local neurons is included, the model exhibits a gain modulation effect that is better described as input-gain control. We apply these findings to experimental data by examining how noisy synaptic input may underlie divisive surround suppression and attention-driven gain modulation of neuronal responses in the visual system.

INTRODUCTION

Gain modulation, often described as a multiplicative or divisive scaling of a neuron's tuning curve, refers to the modification of a neuron's sensitivity to a change in input. Murphy and Miller (2003) have pointed out that "subtractive" mechanisms of inhibition may seem to multiplicatively scale a tuning curve, for example, when there is a nonlinear relationship between stimulus parameters and firing rate. Here we compare the effectiveness of subtractive and divisive mechanisms of inhibition at producing multiplicative/divisive effects on tuning curves recorded in vivo.

We distinguish between subtractive and divisive mechanisms of inhibition according to their actions on firing rate curves (firing rate as a function of input current) of single neurons. Previous studies have shown that noisy background synaptic activity divisively scales the firing-rate curves of individual neurons (Chance et al. 2002; Doiron et al. 2001; Fellous et al. 2003; Mitchell and Silver 2003; Prescott and De Koninck 2003; Shu et al. 2003a). Briefly, increasing the rate of excitatory and inhibitory synaptic inputs together results in increased input current variance, decreasing the slope of the firing rate curve. When combined with an appropriate increase of membrane conductance, the resulting effect is divisive inhibition of the firing rates of single neurons (Fig. 2*A*).

Subtractive inhibition shifts the firing rate curve of a neuron (Fig. 2, *B* and *C*). Shunting, defined here as a tonic membrane conductance with a reversal potential equal to the neuron's resting potential, has a subtractive effect on the firing rate curve of a neuron (Chance et al. 2002; Holt and Koch 1997; Ulrich 2003; also see Fig. 2B) that is very similar to the effect of constant injected current (Fig. 2*C*).

Other studies have proposed that conductance changes underlie the divisive effects on the response functions of neurons, for example, the contrast-response curves (Carandini and Heeger 1994; Carandini et al. 1997; Murphy and Miller 2003) of neurons in primary visual cortex (V1). We will explore the possibility that, although a mechanism is subtractive (defined as shifting the firing-rate curve of a neuron), its effect may appear divisive when neuronal responses are expressed as a function of an external stimulus (Murphy and Miller 2003). We incorporate subtractive and divisive mechanisms of inhibition into a model based on the "normalization model" (Carandini and Heeger 1994; Carandini et al. 1997; Heeger 1992, 1993; Tolhurst and Heeger 1997) and examine whether they can reproduce realistic gain modulation effects on model neuron response curves.

We focus on two types of response curves, which we refer to as tuning curves and intensity curves. Tuning curves describe the neuron's response as a function of a particular stimulus parameter, for example, the orientation of a visual stimulus. Intensity curves describe the neuronal responses as a function of stimulus intensity, such as the contrast of a visual grating pattern. Although both types of response functions describe the neuron's selectivity for a particular stimulus property, in our model, changing stimulus intensity modifies the strength of the drive to a population of neurons, whereas changing a stimulus parameter alters the driven population of neurons.

Finally we compare the effects of these inhibitory mechanisms in our model to gain modulation effects observed in vivo. We focus on two effects, observed in the visual system, which are commonly described as divisive. First, a neuron's response to a visual pattern placed in its receptive field can be suppressed by visual stimuli placed in the area surrounding the receptive field (Allman et al. 1985; Anderson et al. 2001; Blakemore and Tobin 1972; Cavanaugh et al. 2002a; DeAngelis et al. 1994; Dreher 1972; Hubel and Wiesel 1968; Levitt and Lund 1997; Nelson and Frost 1985; Ozeki et al. 2004; Palmer and Nafziger 2002; Sceniak et al. 2001; Sillito et al. 1995). This effect, referred to as "surround suppression," is reported to be stronger when the suppressive stimuli have similar orientation and spatial frequency (Blakemore and Tobin 1972; Cavanaugh et al. 2002b; DeAngelis et al. 1994;

Address for reprint requests and other correspondence: F. Chance, 2205 McGaugh Hall, Univ. of California, Irvine, CA 92697-4550 (E-mail: fchance@uci.edu).

The costs of publication of this article were defrayed in part by the payment of page charges. The article must therefore be hereby marked "*advertisement*" in accordance with 18 U.S.C. Section 1734 solely to indicate this fact.

Gilbert and Wiesel 1990; Levitt and Lund 1997; Nelson and Frost 1978) to the driving stimulus.

Second, the effect of attention is often described as gain modulation (Reynolds and Chelazzi 2004; Salinas and Thier 2000; Treue 2001 for reviews). Of particular interest to this study, the effect is sometimes described as response-gain modulation (McAdams and Maunsell 1999; Treue and Martínez-Trujillo 1999; Williford and Maunsell 2006), where the neuronal response is multiplicatively scaled, and sometimes as input-gain modulation (Martínez-Trujillo and Treue 2002; Reynolds and Desimone 1999; Reynolds et al. 2000), better fit by multiplicatively scaling the input (see Fig. 4, *E* and *F*). We examine how both can be produced in our model, depending on the configuration of inhibition between populations of neurons.

METHODS

Model

In our model, local cortical activity drives different mechanisms of inhibition, which in turn affect the model neuron response curve. We seek to examine how the choice of inhibitory mechanism alters the effect on the response curve. To achieve this goal, we study the responses of a single-compartment leaky-integrate-and-fire (LIF) neuron, representing a cortical neuron. The model neuron is under constant bombardment by excitatory and inhibitory synaptic inputs, as is typical of in vivo cortex (Holt et al. 1996). The membrane potential (V) of the neuron is determined by

$$C\frac{dV}{dt} = g_L[V_L - V(t)] + g_e[E_e - V(t)] + g_i[E_i - V(t)] + I_{FF}(t)$$

In the absence of any synaptic input or additional input currents, the membrane conductance, g_L, is 20 nS, and the membrane time constant, $\tau_L = C/g_L$, is 37 ms, where C is the membrane capacitance of the neuron. The resting membrane potential, V_L, is –70 mV. If the membrane potential V depolarizes above a threshold membrane potential ($V_{th} = -52$ mV), an action potential is fired, and the membrane potential is reset to V_L. I_{FF} is input current representing stimulus-driven feedforward input.

The model neuron receives noisy background synaptic input designed to mimic in vivo conditions. Excitatory and inhibitory synaptic inputs are modeled as incoming spike trains representing the firing of local presynaptic populations of excitatory and inhibitory neurons. The spike times are generated using a Poisson process with underlying input rates of R_e and R_i for excitatory and inhibitory inputs, respectively. With each incoming spike, the excitatory or inhibitory synaptic conductance (g_e and g_i, respectively) instantaneously increases by $0.16g_L$ for excitatory synapses and $0.48g_L$ for inhibitory synapses. In between input spikes, the excitatory and inhibitory synaptic conductances exponentially decay toward zero with a time constant of 5 ms. The unitary sizes of these synaptic inputs, which may represent the arrival of several smaller synchronous synaptic inputs, were chosen so that the resulting subthreshold model membrane potential fluctuations (SD of 2.3 mV) were within ranges observed in vivo (Anderson et al. 2000; Destexhe and Paré 1999; Finn et al. 2007; Paré et al. 1998). The reversal potentials of the excitatory (E_e) and inhibitory (E_i) conductances are 0 and –80 mV. In the absence of any additional input, the average membrane potential is −65.3 mV.

The model neuron always receives a minimum background level ($B = 250$ Hz) of excitatory and inhibitory synaptic input. In the presence of this background activity, the overall membrane conductance is $1.8g_L$, similar to the estimated effect of in vivo background activity (Bernander et al. 1991; Destexhe and Paré 1999; Hirsch et al. 1998; Paré et al. 1998). When examining noisy synaptic input as a mechanism of inhibition, an additional component of noisy synaptic input varies with local cortical activity. We also consider the effects of a shunting conductance, g_{shunt}, that has a reversal potential equal to the resting membrane potential of the neuron, and an injected hyperpolarizing current, I_{inh}, that does not affect the total membrane conductance of the model. With these forms of inhibition included, the membrane potential is determined by

$$C\frac{dV}{dt} = g_L[V_L - V(t)] + g_e[E_e - V(t)] + g_i[E_i - V(t)] + g_{shunt}[V_L - V(t)] + I_{FF}(t) + I_{inh}$$

With the minimum background level of excitatory and inhibitory synaptic input, the effective membrane time constant is 20.5 ms. When cortical activity drives noisy synaptic input or activates shunting conductance, the effective time constant will be shorter.

Feedforward input

The stimulus that drives the feedforward input is referred to as the test stimulus. Feedforward input, I_{FF}, to the model neuron depends on two test stimulus properties, stimulus intensity, c, and a second stimulus parameter, p. For simplicity, we initially assume that I_{FF} increases linearly with increasing stimulus intensity

$$I_{FF} = Lce^{-((p-\alpha)2/\sigma^2)}$$

where $L = 3$ nA for Figs. 3, 4, and 6. In this study, we use the range [0,1] for both c and p. α is the preferred stimulus parameter of the model neuron and equals 0.5, and σ determines the bandwidth of the tuning function and is 0.4 unless otherwise stated.

I_{FF} is constant over time, and the model neuron response is measured as mean firing rate. One exception occurs in Fig. 5, where I_{FF} oscillates in time and neuronal response is quantified by measuring the Fourier component (F1) of the model spike train at the oscillation frequency of I_{FF}.

Cortical inhibition

The model neuron also receives inhibition that is driven by the pooled local activity of cortical neurons (Fig. 1). We consider three mechanisms of cortical inhibition by which this local activity acts on the model neuron: noisy synaptic input, shunting, and hyperpolarizing current. Note that, although these inputs are referred to as "cortical

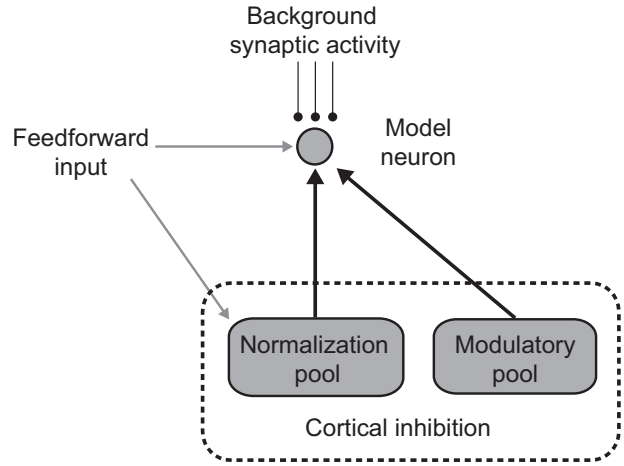

FIG. 1. Cartoon of model circuitry. Feedforward input (gray arrows) drives both the model neuron (gray circle) and the normalization pool. The normalization pool, in turn, inhibits the model neuron (thick black arrow). In addition, the model neuron receives inhibitory input from a modulatory pool of neurons, as well as a background of excitatory and inhibitory synaptic inputs (*top*).

inhibition," they are not comprised solely of inhibitory interneurons. We use this nomenclature because the inputs originate in cortex and have a suppressive effect on the firing rate of the model neuron.

The local cortical activity is divided into two pools of neurons: the "normalization pool" and the "modulatory pool." The normalization pool is based on the normalization model proposed by Heeger (1992, 1993). Normalization pool activity, a_N, is driven by the feedforward input (Fig. 1, gray arrows) and thus is a function of stimulus intensity

$$a_N \propto c^{1.5}$$

We set the normalization pool activity to vary supralinearly with stimulus intensity because this produced more realistic intensity-response curves (see Fig. 3). We assume that the normalization pool includes neurons with a wide range of stimulus selectivities and that the receptive fields of these neurons are located in a similar region as the model neuron. Because of the wide range of stimuli, normalization pool activity is assumed to remain constant as test stimulus parameter p is varied, but it depends on the test stimulus intensity, c. The modulatory pool may be thought of as a pool of neurons driven by a stimulus located outside the receptive field of the model neuron or by some other modality, such as the behavioral state of the animal. The activity level of this neuron pool is a_M

$$a_M \propto k$$

where k describes the stimulus that drives the modulatory pool. We refer to this stimulus as the modulatory stimulus.

Initially (in Fig. 3) we consider the case where the normalization pool and the modulatory pool are driven independently of each other. The total activity of the cortical pool is

$$A = c^{1.5} + Mk$$

where the parameter M determines the relative contributions of the normalization pool and the modulatory pool to total cortical activity. For Fig. 3, *B* and *E,* (when cortical inhibition activates a shunting conductance), $M = 0.1$. For all other panels in Figs. 3 and 4, $M = 0.2$.

When the mechanism of cortical inhibition is noisy synaptic input, the rates of the noisy excitatory (R_e) and inhibitory (R_i) synaptic input depend on the activity of the two cortical pools

$$R_e = R_i = JA + B$$

where A is total cortical activity as described above, B is the baseline background activity defined earlier, and $J = 5{,}750$ Hz for Figs. 3 and 4. When cortical inhibition acts through a shunting conductance, the conductance magnitude depends on the activity of the cortical pool

$$g_{shunt} = JA$$

For shunting conductance in Figs. 3 and 4, $J = 6.15g_L$. Finally, when local cortical activity drives additional hyperpolarizing injected current, that current depends on the activity of the two cortical pools

$$I_{inh} = JA$$

where $J = -1.68$ nA (for Figs. 3 and 4).

Interactions between the normalization pool and the modulatory pool activity

In Fig. 4, we include reciprocal inhibition between the normalization pool and the modulatory pool (see illustration in Fig. 4*A*)

$$a_N = \frac{1}{1 + 1.25a_M}c^{1.5} \quad \text{and} \quad a_M = \frac{1}{1 + 1.25a_N}Mk$$

where a_N is the activity of the normalization pool, and a_M is the activity of the modulatory pool. To determine total cortical activity in response to a given test stimulus (of intensity c) and modulatory stimulus k, we first ran an iterative subroutine to allow the values of a_N and a_M to converge. Total cortical pool activity, A, is the sum of these values, $a_N + a_M$, and noisy synaptic input rates, shunting conductance, and hyperpolarizing current were calculated as described above.

Surround suppression model

The model in Fig. 5 represents a neuron in primary visual cortex (V1) responding to a "test" patch of drifting sinusoidal grating placed in the cell's receptive field and an annulus grating surrounding the receptive field of the neuron. The test grating is assumed to be of the preferred spatial frequency and orientation of the model neuron and drives both the normalization pool activity and the feedforward input to the neuron. Because it is outside of the receptive field of the model neuron, we assume that the "surround" grating does not affect the feedforward input to the neuron, but instead only drives the activity of the modulatory pool.

In this example, the feedfoward input (I_{LGN}) arises from the lateral geniculate nucleus (LGN) and is a sinusoidal oscillating input current (reflecting the sinusoidal pattern of the drifting grating)

$$I_{LGN}(t) = L\sin(\omega t)\frac{c_{test}^{1.5}}{c_{test}^{1.5} + \lambda^{1.5}}$$

where $c \in [0,1]$ and ω (6 Hz) are the contrast and the temporal frequency of the test grating, respectively. For this example, the parameter L was adjusted so that the magnitudes of the model responses were similar to those measured in V1. The amplitude of the LGN input saturates with contrast and the value of the semisaturation constant, $\lambda = 0.3$, was chosen to be similar to reported values (Derrington and Lennie 1984; Finn et al. 2007; Li et al. 2006) measured in in vivo LGN. Because the model neuron is driven by an oscillating stimulus, the firing rate response will also oscillate in time. For this figure, we quantify the response of the neuron to drifting gratings by measuring the Fourier component (F1) of the model spike train at stimulus frequency ω. This is essentially the amplitude of the firing rate modulation and is a standard method of reporting the response of a V1 simple cell to sinusoidally oscillating stimuli such as drifting gratings.

The model V1 neuron also receives input from the normalization pool, which is thought to consist of a population of local V1 neurons with receptive fields in a similar location to the model neuron, but with a wide range of stimulus selectivities (Heeger 1992, 1993). Because this pool contains neurons with all possible spatial phase preferences, the population activity is time invariant. The modulatory pool consists of V1 neurons, also with a wide range of stimulus selectivities, with receptive fields located in the visual area occupied by the surround grating. Similar to the normalization pool, the activity of the modulatory pool in response to the surround stimulus is constant in time.

Because of the locations of their receptive fields, the normalization pool is driven by the test grating and the modulatory pool by the surround grating. The saturating contrast-response function of V1 neurons is often described as a hyperbolic ratio function (Albrecht and Hamilton 1982; Contreras and Palmer 2003; Sclar et al. 1990) or the Naka-Rushton function (Albrecht and Hamilton 1982; Chao-yi and Creutzfeldt 1984; Naka and Rushton 1966). We describe the normalization pool activity (a_N) and the modulatory pool activity (a_M) as saturating functions of the test (c_{test}) and surround ($c_{surround}$) grating contrasts

$$a_N = \frac{c_{test}^{1.5}}{c_{test}^{1.5} + 0.6^{1.5}} \quad \text{and} \quad a_M = \frac{c_{surround}^{1.5}}{c_{surround}^{1.5} + 0.6^{1.5}}$$

where a_N and a_M are the activities of the normalization and the modulatory pool, respectively. The rates of noisy excitatory (R_e) and inhibitory (R_i) synaptic input are

$$R_e = R_i = JA + 1000 \text{ Hz},$$

where J = 9,000 Hz and A (equaling $a_N + a_M$) is the total cortical pool activity.

In Fig. 5*B*, we include reciprocal inhibition between the population of normalization pool neurons tuned for the test stimulus and the population of normalization pool neurons responsive to surround stimulus. The contrast-response functions of these populations are now

$$a_N = \frac{1}{1 + 1.75a_M}\left(\frac{c_{test}^{1.5}}{c_{test}^{1.5} + 0.5^{1.5}}\right) \quad \text{and}$$

$$a_M = \frac{1}{1 + 1.75a_N}\left(\frac{c_{surround}^{1.5}}{c_{surround}^{1.5} + 0.5^{1.5}}\right)$$

For each pair of stimuli, we first ran an iterative subroutine to allow the values of a_N and a_M to converge. Noisy synaptic input rate was calculated as described above, except with J = 11,000 Hz.

Attention model

In Fig. 6, we examine how varying the strength of reciprocal inhibition can produce different modulatory effects. We examine the effect of the two different levels of modulatory pool activity on model tuning curves.

We use the same model of feedforward input as for Fig. 3

$$I_{FF} = Lce^{-((p-\alpha)^2/\sigma^2)}$$

where c is stimulus intensity (e.g., the contrast of a visual stimulus), p is a stimulus parameter (i.e., stimulus orientation), L = 3 nA, α = 0.5, and σ = 0.3. For the simulations in Fig. 6, c = 1. The normalization pool input to the model neuron also is tuned for the stimulus

$$a_N = c^{1.5}e^{-((p-\alpha)^2/\sigma^2)}$$

The modulatory pool activity, driven by attention or the behavioral state of the animal, is independent of the external stimulus

$$a_M = Mk$$

and drives noisy synaptic activity. For Fig. 6*A*, normalization pool and modulatory pool activity are independent of each other and the synaptic input rates are

$$R_e = R_i = 250 + J(a_N + a_M)$$

In Fig. 6*A*, J = 6,000, M = 0.05, and k = 1 or 6 for the attended or unattended state, respectively.

In Fig. 6*B* we include reciprocal inhibitory interactions between the normalization pool and the modulatory pool. Now

$$a_N = \frac{c^{1.5}}{1 + Da_M}e^{-((p-\alpha)^2/\sigma^2)} \text{ and } \quad a_M = \frac{1}{1 + Da_N}Mk$$

where D = 1.825 is a parameter that describes the strength of the reciprocal inhibition between the cortical pools. In Fig. 6*C*, we consider a stronger inhibitory interaction between cortical pools and set D = 2.5. For Fig. 6, *B* and *C*, α = 0.5, σ = 0.3, M = 0.1, and k = 1 or 8 for the unattended and the attended state, respectively. Excitatory and inhibitory synaptic input rates are the same as for Fig. 6*A*, except that J = 6,500.

RESULTS

We define divisive and subtractive mechanisms of inhibition based on their impact on neuronal firing rate curves. The filled squares in Fig. 2 are the firing-rate curve of the model neuron with excitatory and inhibitory synaptic input rates set to 1,000 Hz (Fig. 2*A*). In Fig. 2*A*, we show the effects of increasing this noisy synaptic input by increasing the noisy synaptic input rate to 2,500 open squares and 4,000 Hz filled triangles. The dominant effect of increasing the noisy excitatory and inhibitory synaptic input is a divisive scaling of the firing rate curve. To show this, we fit the open squares with the best fourth-order polynomial fit (thick curve) and multiplicatively scaled the polynomial fit to produce the thinner curves.

In Fig. 2*B*, rather than increase noisy synaptic input, we introduce a tonic shunting conductance (with a reversal potential equal to the resting membrane potential) into the model neuron membrane. Increasing this conductance to $1.25g_L$ and $2.5g_L$ (g_L is the resting membrane conductance of the neuron) shifts the firing rate curve of the neuron cf. open squares and filled triangles to filled squares. We show the subtractive effect of this mechanism of inhibition by again determining the best fourth-order polynomial fit to the open squares (thick curve) and shifting it along the input axis (thinner curves). Because

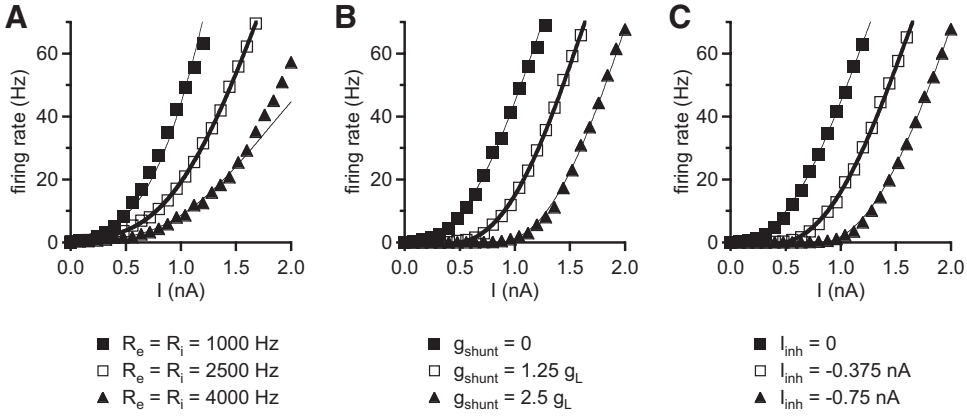

FIG. 2. Effects of different inhibitory mechanisms on model firing-rate curves. For all panels, the filled squares are the firing-rate curve of the model neuron receiving 1,000-Hz noisy synaptic input, and the thick curve is the best 4th-order polynomial fit of the data drawn with open squares. *A*: the arrival rates of excitatory and inhibitory inputs were increased to 2,500 (□) and 4,000 Hz (▲), as indicated in the legend. The thinner curves are multiples (2.3× and 0.45×) of the thick curve. *B*: model firing-rate curves with an additional shunting conductance equal to $1.25g_L$ (□) and $2.5g_L$ (▲). The thinner curves were produced by shifting the thick curve by −0.37 or 0.39 nA. *C*: to produce the firing-rate curves described by □ and ▲, −0.375 and −0.75 nA of constant injected current was applied (in addition to that indicated on the *x*-axis). The thin curves are shifted (by −0.375 or +0.375 nA) versions of the thick curve.

these curves are approximately linear at high firing rates, distinguishing a horizontal shift along the input axis from a vertical shift along the response axis is not possible, except at low rates where the shape of the firing rate curve is determined by the noisy synaptic input. We will revisit this issue when we discuss Fig. 3.

For comparison with the effect of shunting conductance, we also examine the effect of injecting hyperpolarizing current. The two firing rate curves in Fig. 2*C* marked by open squares and filled triangles were produced by injecting constant hyperpolarizing current in addition to the driving current plotted on the *x*-axis. Because injecting additional input current is equivalent to shifting the firing-rate curve along the *x*-axis, the subtractive effect on the firing-rate curve is not surprising. As in Fig. 2*B*, the thick curve is the best fourth-order polynomial fit to the open squares and the thinner curves were produced by shifting this fit along the input axis.

Having distinguished between divisive and subtractive mechanisms of inhibition based on their effects on firing rate curves, we now seek to examine the effects of these mechanisms on response tuning curves. The model neuron receives two types of input: input current that represents feedforward stimulus-driven input originating from an earlier stage of processing and suppressive or inhibitory input arising from pooled local cortical activity that acts through one of the three inhibitory mechanisms described in Fig. 2. As described in METHODS, the Gaussian-shaped tuning curve of the model neuron arises from the feedforward input, I_{FF}, a function of a stimulus parameter, p, and stimulus intensity, c

$$I_{FF} = Lce^{-((p-\alpha)^2/\sigma^2)}\text{nA}$$

For simplicity, the feedforward input increases linearly with stimulus intensity (except for Fig. 5, see METHODS for details).

The inhibitory or suppressive input is driven by activity in two cortical "pools" of neurons (Fig. 1). The normalization pool is much like the normalization pool proposed by Heeger and colleagues (Carandini et al. 1997; Heeger 1992, 1993) and encompasses neurons with a wide range of stimulus preferences. The modulatory pool is driven by a different stimulus than the normalization pool. For clarity, we refer to the stimulus that drives the modulatory pool as the modulatory stimulus (although it may be driven by factors such as the behavioral state of the animal as well as external stimuli) and the stimulus that drives the normalization pool as the test stimulus.

Because the normalization pool is driven by feedforward input, its activity increases with test stimulus intensity, c. We set normalization pool activity to increase with $c^{1.5}$ because this created intensity-response curves with realistic saturation effects. However, because we assume the normalization pool contains neurons tuned for every possible value of test stimulus parameter p, normalization pool activity is independent of p. The modulatory pool activity is driven by the modulatory stimulus and is independent of the test stimulus. Cortically generated inhibition increases proportionally with the sum of the normalization and the modulatory pool activities.

We consider three cases in which local cortical activity leads to increased noisy synaptic activity (Fig. 3, *A* and *D*), increased shunting conductance (Fig. 3, *B* and *E*), or increased hyperpolarizing current (Fig. 3, *C* and *F*) and examine its effect on the model tuning curves (for details, see METHODS). Figure 3, *A–C,* shows stimulus tuning curves of the model neurons. Each curve is the firing rate of the model neuron as a function of test stimulus parameter p. The filled squares, open squares, and filled triangles in each panel are the tuning curves with a different modulatory stimulus. For Fig. 3*A*, the test stimulus and the modulatory stimulus drove increases in noisy synaptic input rate. Within each tuning curve, normalization pool and modulatory pool activities are constant, and only the feedforward input changes as a function of the stimulus parameter. As expected, increasing the modulatory stimulus (and thus cortical inhibition) decreased the firing rate of the model neuron. The dominant effect is a divisive scaling of the tuning curve.

The effect of the subtractive mechanisms of inhibition, shunting conductance (Fig. 3*B*), and hyperpolarizing injected current (Fig. 3*C*) is different. As in Fig. 3*A*, the level of cortical inhibition is constant for each tuning curve, and increasing cortical inhibition decreases the model neuron responses. For subtractive mechanisms of inhibition, however, the decrease in

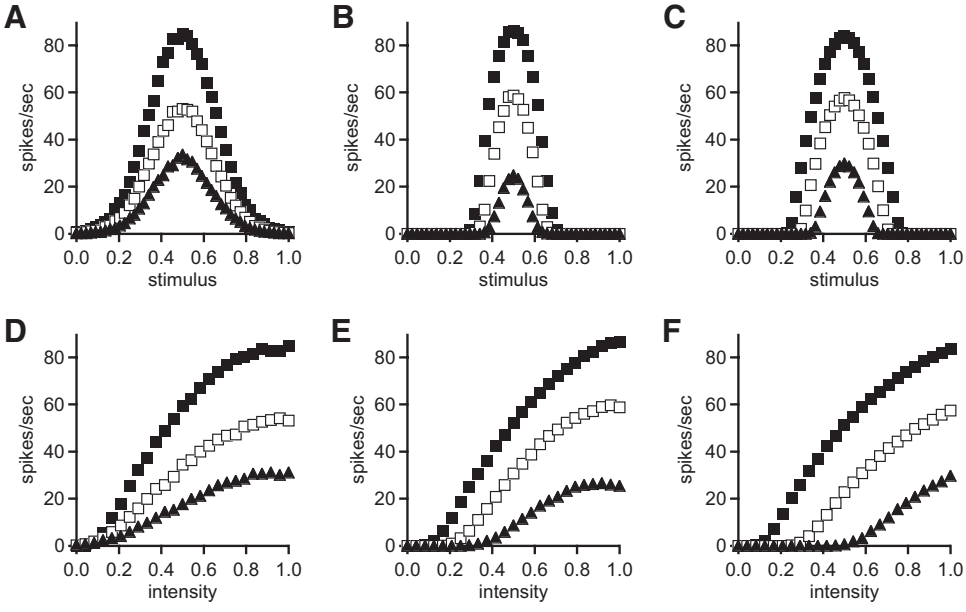

FIG. 3. Tuning and intensity curves of model neuron responses for different modulatory stimuli. Cortical inhibition pool activity increased either noisy synaptic input (*A* and *D*), shunting conductance (*B* and *E*), or hyperpolarizing current (*C* and *F*). For all panels, modulatory stimulus $k = 0$ (■), 1 (□), or 2 (▲). The preferred stimulus of the neuron was $\alpha = 0.5$. *Top panels* (*A–C*): model firing rate as a function of test stimulus parameter (labeled stimulus) and test stimulus intensity $c = 1$, for the 3 different modulatory stimuli. *Bottom panels* (*D–F*): model firing rates as a function of test stimulus intensity c (with stimulus parameter 0.5) for the 3 different modulatory stimuli. Noisy synaptic input rates were 250 Hz in *B, C, E,* and *F*.

model responses is accompanied by a narrowing of the tuning curve. This narrowing is particularly conspicuous when examining what range of p the neuron is responsive to for a given modulatory stimulus.

Figure 3, *D–F,* shows stimulus-intensity curves (firing rate as a function of test stimulus intensity c) for the same modulatory stimuli as in Fig. 3, *A–C*. In this case, although the component of cortical inhibition resulting from the modulatory stimulus is constant, the cortical inhibition driven by the test stimulus increases with test intensity. The intensity curves in Fig. 3*D* resulted when cortical activity drove increases of noisy synaptic input. As expected, model neuron firing rate increases with stimulus intensity. However, the response curve saturates above a particular stimulus intensity, even though the feedforward input is a linear function of stimulus intensity. This nonlinearity in the intensity curve occurs because cortical inhibition increases more rapidly with stimulus intensity than with feedforward input.

As for Fig. 3*A*, the dominant effect of increasing the modulatory stimulus in Fig. 3*D* is a divisive scaling of the intensity curve. This divisive effect is an example of response-gain control. That is, the divisive effect acts on the responses of the model neuron. In Fig. 4, we consider how interactions between cortical pools can give rise to input-gain control, where the divisive effect acts on the input variable.

Figure 3, *E* and *F,* shows model intensity-response curves when the mechanism of inhibition is shunting conductance and hyperpolarizing current, respectively. By comparing these panels, it is clear that the divisive mechanism of inhibition has a different effect than the subtractive mechanisms of inhibition. When a subtractive mechanism is used, the dominant effect on the contrast-response curve is a subtractive shift. In particular, the modulatory stimulus introduces a definite shift in response threshold.

Closer inspection of the intensity-response curves in Fig. 3, *E* and *F,* shows that the effects of the subtractive mechanisms of inhibition are better described as a vertical shift of the response curve along the response axis rather than a horizontal shift along the input axis. In some cases, particularly when the responses are low, this shift can appear to be accompanied by a change in slope. This apparent change in gain arises because of the nonlinear shape of the intensity-response curve and the presence of noisy synaptic input. Because it is a saturating function, the slope of the intensity-response function decreases with higher levels of test intensity. As the modulatory stimulus increases, the intensity-response function is shifted downward, bringing the lower-gain portion of the response function closer to response threshold. Thus a vertically shifted intensity-response function may seem to have undergone a divisive scaling if the shift in response threshold is not noted. Furthermore, the background level of noisy synaptic input present in all simulations will soften the response threshold of a neuron and obscure the shift in response threshold.

The intensity-response functions of cortical neurons tend to saturate at high intensities (Tolhurst and Dean 1991). In our model, the intensity-dependent saturation of the response curves arises because the cortical pool activity (and hence suppression of model firing rate) rises faster than the feedforward input to the model. Other nonlinearities, for example, a saturating feedforward-input function, will also produce this effect. This nonlinearity does not qualitatively change the effect of the modulatory pool activity for any mechanism of inhibition, although it does make distinguishing between the different effects more difficult. The effects of noisy synaptic input (Fig. 3, *A* and *D*), shunting conductance (Fig. 3, *B* and *E*), and hyperpolarizing current (Fig. 3, *C* and *F*) can appear very similar when the stimulus is in a regimen where the intensity-response curve is saturated (where the neuron's response is relatively independent of intensity). Determining whether a response curve is vertically shifted or divisively scaled is particularly difficult in cases where the intensity curve saturates relatively early and the curve is mainly horizontal. In these cases, the most significant differences between effects of different inhibitory mechanisms will occur at lower contrasts where the curves are not saturated.

We have shown that, although subtractive and divisive inhibitory mechanisms can produce similar effects on the tuning curves and intensity-response curves of neurons (in fact, the intensity-dependent saturation effects arising from divisive and subtractive inhibition are indistinguishable from each other), only suppression acting through divisive inhibition produces response-gain modulation. We assumed that the activity of the normalization pool is independent of the modulatory pool activity, an assumption that is valid only if the test and modulatory stimuli act through independent channels, for example, if they drive independent pools of cortical neurons (as in our model).

Some studies have reported input-gain modulation effects by modulatory stimuli. For example, the effects of attention may modify the contrast gain of neurons in V4 (Reynolds et al. 2000) and also MT (Martínez-Trujillo and Treue 2002). Because it is input gain that is being modified (equivalent to scaling the input variable), such an effect is referred to as input-gain modulation. We can produce input-gain modulation in our model by including interactions between the normalization pool and the modulatory pool. To illustrate this effect, we now extend our model to include reciprocal inhibition between the populations of neurons (Fig. 4*A*). Although the two pools are still driven independently of each other, the activity of each population divisively inhibits the activity of the other. This inhibition is hard-coded into the model (see METHODS for details).

Figure 4*B* shows how incorporating reciprocal inhibition between the modulatory and the normalization pool affects their activities. In the *top panel* of Fig. 4*B*, normalization pool activity is plotted as a function of test stimulus intensity. The solid curve is the normalization pool activity when only the test stimulus is presented. The dotted curve and dashed curve represent the test pool activity when the modulatory stimulus was 1 (dotted curve) or 2 (dashed curve) and differ from the solid curve because of inhibition from the modulatory pool. The *middle panel* of Fig. 4*B* is modulatory pool activity as a function of test stimulus intensity when the modulatory stimulus is zero (the solid line at the bottom of the plot indicates that modulatory pool activity is 0 (when there is no modulatory stimulus), 1 (dotted line), or 2 (dashed line). In the absence of interactions between pools, all modulatory pool activity curves should be flat. However, because of the reciprocal inhibitory interactions between pools, the modulatory pool activity decreases as test stimulus intensity increases.

Total cortical activity is plotted as a function of test stimulus contrast in the bottom panel of Fig. 4*B*. Again, the solid curve

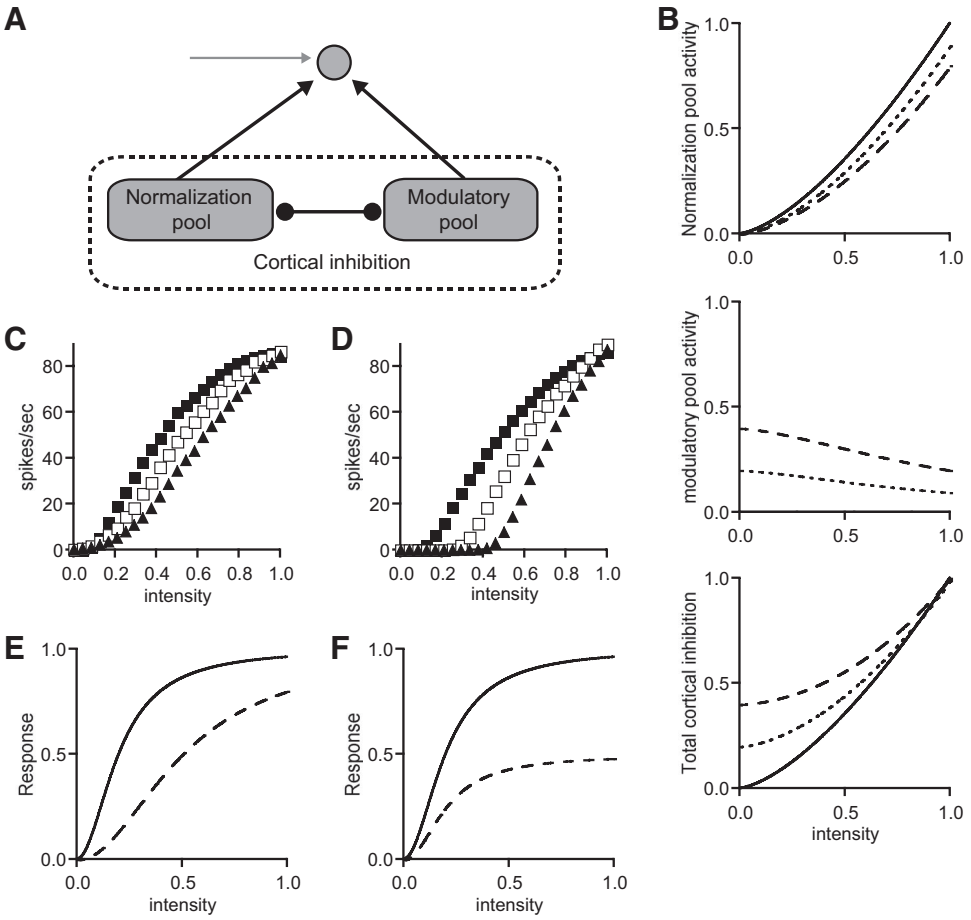

FIG. 4. Model intensity-response curves with reciprocal inhibition included between normalization and modulatory pools. *A*: the model is very similar to that described in Fig. 1, except that reciprocal inhibition between the normalization pool and the modulatory pool is included. *B*: normalization (*top*), modulatory (*middle*), and total (*bottom*) pool activity as a function of test stimulus intensity. In each panel, the modulation stimulus was 0 for solid curves, 1 for dotted curves, and 2 for dashed curves. *C*: model neuron firing rates as a function of test stimulus intensity when noisy input rates arise from the total pool activity described in *B*. Modulation stimulus was 0 (■), 1 (□), and 2 (▲) in *C* and *D*. *D*: model intensity-response curves when total pool activity drives increases in shunting conductance. *E*: example of input-gain control. The solid curve is $x^2/(0.2^2 + x^2)$, with x representing stimulus intensity. The dotted curve is $x^2/(0.4^2 + x^2)$. *F*: example of response-gain control. The solid curve is identical to the solid curve in *E*. The dotted curve is the solid curve divided by 2.

represents activity for no modulatory stimulus, and the dotted and dashed lines are total cortical pool activity when the modulatory stimulus is 1 and 2. The model intensity-response curves that resulted when these curves determined the noisy synaptic input rates (see METHODS) are given in Fig. 4*C*. The filled squares are model responses to a test stimulus of the intensity indicated on the *x*-axis. Open squares and filled triangles are model responses when the modulatory stimulus was 1 and 2, respectively. With reciprocal inhibition included, the modulatory stimulus has a different effect on the intensity-response curves (cf. Fig. 4*C* with Fig. 3*D*). Although at low test stimulus intensities the effect of cortical inhibition through increased noisy synaptic input appears divisive, the firing rate curves in Fig. 4*C* saturate at similar maximum firing rates. This effect is closer to a scaling of the intensity variable rather than a scaling of the model responses.

If cortical activity instead drives a subtractive mechanism of inhibition, the effect on the intensity-response curves is different. In Fig. 4*D*, cortical inhibition acts by increasing shunting conductance. As in Fig. 4*C*, the filled squares are model firing rates in the absence of a modulatory stimulus, and the open squares and solid triangles are firing rates when the modulatory stimulus is 1 and 2. As in Fig. 3*E*, increased shunting conductance led to an increased intensity threshold for a response. This cannot be described as a divisive effect.

With reciprocal inhibition included, the effect of the modulatory stimulus is best described as a divisive scaling of the intensity variable when cortical inhibition acts through noisy synaptic input (Fig. 4*C*). This effect is often referred to as "input-gain control." A cartoon of this effect is shown in Fig. 4*E*, where the intensity variable of a hypothetical intensity-response function (solid curve) is divided by a constant factor to produce the second intensity-response function (dashed curve). Alternatively, in Fig. 3*D*, the divisive effect of noisy synaptic input acts on the model firing rates. A cartoon of this effect is shown in Fig. 4*F*, where the solid intensity-response curve was divided by a constant factor to produce the dashed curve. Because the neuronal responses are scaled, this effect is often referred to specifically as "response-gain control."

When the cortical pool activities are independent of each other (Fig. 3), response-gain modulation (divisive scaling of neuronal responses) only arises when the inhibitory mechanism is noisy synaptic input. Furthermore, we only observed input-gain modulation (divisive scaling of the input variable) when the inhibitory mechanism was noisy synaptic input and reciprocal inhibition was included between the cortical pools. We now examine how noisy synaptic inputs, arising from local cortical circuitry, give rise to gain modulation effects observed in cortex, specifically within the visual system. In Fig. 5, we compare model responses to surround suppression effects observed in primary visual cortex (V1), and in Fig. 6, we compare model responses to attention effects observed in V4 and area MT.

Figure 5 shows the responses of a model V1 simple cell to two simultaneously presented drifting sinusoidal gratings. The test grating is a patch of drifting grating presented in the

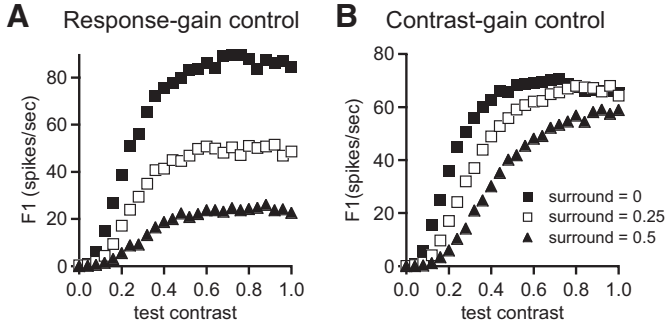

FIG. 5. Surround suppression in the V1 model with response-gain control and contrast-gain control. ■, responses to test stimulus only; □, responses to test stimulus and a surround stimulus of contrast 0.25; ▲, responses to test stimulus and a surround stimulus of contrast 0.5. *A*: responses of the model V1 neuron as a function of test contrast. The activities of the normalization pool and the modulatory pool are independent of each other. *B*: responses of the model V1 neuron when reciprocal inhibition is included between cortical pools.

receptive field of the neuron, and the surround grating is an annulus of drifting grating presented in the region surrounding the receptive field of our model neuron. We assume that both gratings are of the preferred orientation and spatial frequency for the model neuron. In this example, the normalization pool consists of neurons with a wide range of spatial phase, orientation, and spatial frequency preferences, but with receptive fields located in a similar region of space as the model neuron (Carandini et al. 1997; Heeger 1992, 1993). Likewise, the modulatory pool contains neurons with a wide range of selectivities, but whose receptive fields are located in regions adjacent to the receptive field of the model neuron.

As described in METHODS, the feedforward input arising from the LGN is represented as a sinusoidal oscillating input current. We incorporate LGN contrast saturation (Derrington and Lennie 1984; Finn et al. 2007; Li et al. 2006) by setting the amplitude of this oscillating current to be a hyperbolic function of test grating contrast (see METHODS). We assume that LGN activity arising because of the surround stimulus does not directly drive the model V1 neuron. Therefore the feedforward input is unaffected by surround contrast.

In this example, the normalization pool and the modulatory pool both contain V1 neurons with all possible spatial phase preferences but receptive fields in different locations. Thus the activity of each population is time invariant in response to drifting grating stimuli. V1 neuron responses are often modeled as hyperbolic ratio functions of stimulus contrast (Albrecht and Hamilton 1982; Chao-yi and Creutzfeldt 1984; Contreras and Palmer 2003; Sclar et al. 1990). We capture this feature of V1 responses by setting the normalization pool activity and the modulatory pool activity to be saturating functions of test and surround contrast gratings, respectively (see METHODS). Both pools drive cortical inhibition by increasing noisy excitatory and inhibitory synaptic input rates.

We quantify the response of the neuron to drifting gratings by measuring the Fourier component (F1) of the model spike train at stimulus frequency ω. This is essentially the amplitude of the firing rate modulation and is a standard method of reporting the response of a V1 simple cell to sinusoidally oscillating stimuli such as drifting gratings. The filled squares are the responses of the model neuron, measured in this way, as a function of test contrast in the absence of the surround grating ($a_M = 0$). For the open squares and filled triangles, the surround grating contrast was 0.25 and 0.5, respectively. The cortical inhibition driven by the surround grating has a response-gain modulation effect on the model contrast-response curve.

In Fig. 5*B*, we include reciprocal inhibition between the normalization pool and the modulatory pool. The reciprocal inhibition is similar to that used for Fig. 4 (see METHODS for details). As in Fig. 5*A*, the filled squares are the model responses in the absence of a surround stimulus, and the open squares and filled triangles are responses when the surround stimulus contrast is increased to 0.25 and 0.5, respectively. With reciprocal inhibition included between the two cortical pools, the effect of presenting a surround stimulus is now better described as input-gain modulation rather than response-gain modulation (as in Fig. 5*A*).

In Fig. 6, we examine how interactions between the cortical pools can produce different attention-driven gain modulation effects observed in vivo. The feedforward input is driven by the external stimulus as in Fig. 3. As described in METHODS, the normalization pool is also driven by the external stimulus; however, for this example, we also allow normalization pool activity to have the same input selectivity as the model neuron

$$a_N = c^{1.5} e^{-((p-\alpha)^2/\sigma^2)}$$

Tuned normalization pool activity such as this could arise if local recurrent connections are tuned for stimulus selectivities; for example, if visual neurons with similar orientation preferences are more strongly connected than neurons with orthogonal orientation preferences.

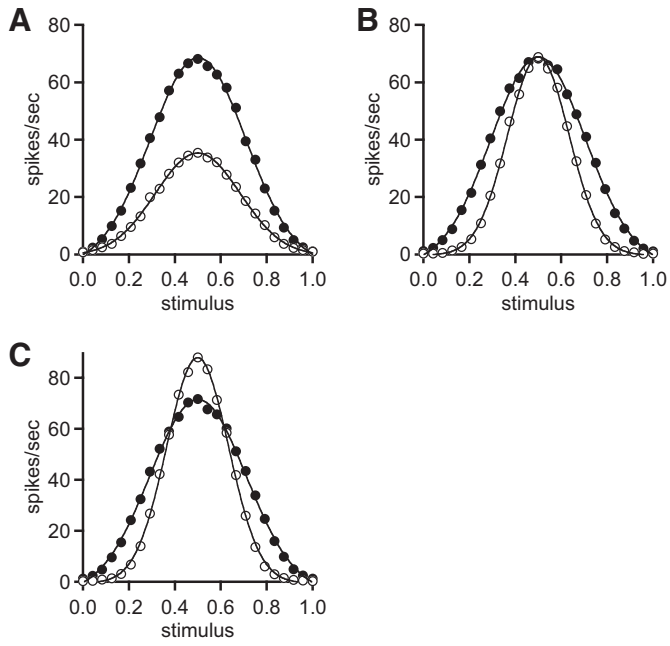

FIG. 6. Model tuning curves for low (●) and high (○) levels of modulatory pool activity. *A*: tuning curves of the model for which normalization pool and modulatory pool activities are driven independently of each other. *B*: tuning curves with reciprocal inhibition included between the normalization and modulatory pool ($D = 1.825$). *C*: tuning curves for stronger reciprocal inhibition included between the normalization and the modulatory pool ($D = 2.5$). Test stimulus intensity, c, was 1. Solid curves are best Gaussian fits to symbols.

For this example, the modulatory pool activity may be thought of as determined by the behavioral state of the animal, such as whether the animal is attending to or away from the receptive field of the model neuron. In Fig. 6*A*, the activity of the normalization pool and the activity of the modulatory pool arise independently, and (as in Fig. 3*A*) noisy synaptic input rates are determined by the sum of the normalization pool activity and modulatory pool activity.

The filled circles in Fig. 6*A* are the model neuron firing rate as a function of the stimulus parameter when modulatory pool activity is low (parameter $k = 1$). When modulatory pool activity is increased ($k = 6$), the increased synaptic activity results in a divisive scaling of the model tuning curve (open circles). For this mechanism to underlie attentional effects, attention must result in a decrease in modulatory pool activity. This would result in less noisy synaptic input and a multiplicative enhancement of the neuronal tuning curve, an effect of attention observed in V4 and also MT (McAdams and Maunsell 1999; Treue and Martínez-Trujillo 1999; Williford and Maunsell 2006). In this scenario, modulatory pool activity increases when attention is directed away.

In Fig. 6, *B* and *C*, we include mutual inhibition between the normalization pool and the modulatory pool. As in previous figures, mutual inhibition is hard-coded into the model (see METHODS for details), with *D* describing the strength of the inhibition between cortical pools. Normalization pool activity, selective for the stimulus parameter, inhibits modulatory pool activity, which is independent of the test stimulus. The modulatory pool activity will be more inhibited when the stimulus is of the preferred parameter (0.5 in this case) and thus has a more significant impact on the flanks of the tuning curve where its activity is higher. Increasing modulatory pool activity will thus lead to a narrowing of the tuning curve or an increase in the selectivity of the model neuron. If the strength of mutual inhibition is appropriately balanced, the narrowing of the tuning curve may be the only observed effect, as in Fig. 6*B*. In this figure (as for Fig. 6*A*), the filled circles are firing rates for low modulatory pool activity ($k = 1$). For the open circles, modulatory pool activity increased ($k = 8$).

Depending on the strength of the mutual inhibition, the narrowing of the tuning curve may be combined with an enhancement of neuronal responses to the preferred stimulus, essentially an even more dramatic enhancement of selectivity. In Fig. 6*C*, *D* was increased to 2.5 (from 1.825 in Fig. 6*B*). The model's responses to preferred stimuli or stimuli very close to the preferred stimuli are enhanced, whereas the model's responses to stimuli far from the preferred stimuli are suppressed. In this panel, attention effectively increases the selectivity of the model neuron. Such an effect has been reported in area MT (Martínez-Trujillo and Treue 2004). If the strength of inhibition is decreased, the tuning curve will again be narrowed, but this narrowing will be combined with an overall decrease in neuronal responses (data not shown).

DISCUSSION

We examined whether the effects of inhibitory mechanisms on the firing rate curves of in vitro neurons may differ from their effects on in vivo response tuning curves. Divisive and subtractive mechanisms of inhibition were classified according to their effects on neuronal firing rate curves. We used increasing levels of noisy synaptic input as a divisive mechanism of inhibition, and shunting and hyperpolarizing current as subtractive mechanisms. When incorporated into our model, only noisy synaptic input produced multiplicative gain modulation of model tuning curves. Also, we found that the type of gain modulation (input-gain control or response-gain control) can be controlled through altering local inhibitory interactions between "pools" of neurons.

One important requirement of noisy synaptic input as a divisive mechanism is the covariance of evoked excitatory and inhibitory synaptic input. Recent findings have shown that in cortex, activations of excitatory and inhibitory synaptic conductances co-vary, whether in slice (Shu et al. 2003b) or visually evoked in cat area 17 (Mariño et al. 2005; Monier et al. 2003), suggesting that in vivo cortical circuitry can generate the necessary configuration of noisy synaptic input. It remains to be seen, however, if excitation and inhibition co-vary in the appropriate manner to underlie surround suppression (Anderson et al. 2001; Ozeki et al. 2004) or attention.

In our studies, shunting was implemented by introducing a tonic conductance change with a reversal potential equal to the resting potential of the neuron. However, shunting does not have to arise from a single conductance, because a combination of tonic excitatory and inhibitory conductances with the effective reversal potential at the resting membrane potential will have the same effect. Noisy excitatory and inhibitory synaptic inputs have a divisive effect on the firing rate curve of a neuron because of the increase in input current variance that accompanies an increase in synaptic input rate. This change does not occur with an increase in constant conductance, and for this reason, shunting is subtractive, not divisive (for a full discussion, see Chance et al. 2002; Holt and Koch 1997; Ulrich 2003).

We incorporated these mechanisms of inhibition, driven by "pools" of local cortical activity, into our model and observed the effects on the response functions of neurons. When the activities of the pools are independent of each other, the divisive mechanism of inhibition produced effects best described as response-gain control, whereas the subtractive mechanisms of inhibition shifted the contrast-response curve downward along the response axis. The differences between the effects of divisive and subtractive mechanisms are most apparent when examining responses close to threshold, as subtractive inhibition increased the response threshold (the level of input required to elicit a response from the model) while divisive inhibition did not affect it. The effects of noisy synaptic input may obscure the shift in response threshold, particularly if the input function increases rapidly close to response threshold. An example of such an input function is a hyperbolic ratio function (Fig. 5; also see Murphy and Miller 2003), with a small semisaturation constant. In addition, if the response curves saturate, it can be difficult to distinguish between divisive and subtractive effects based on the saturating portions of the response curves. Under conditions such as these, subtractive mechanisms can seem to have a divisive effect.

Murphy and Miller (2003) reported that subtractive mechanisms of inhibition may seem to have a divisive effect when there is a nonlinear relationship between stimulus parameter and input current and also between input current and firing rate (as introduced by the presence of background noise). As they

note, in their work, the effect of their modulatory stimulus was relatively small relative to the effect of the driving input. We can reproduce the findings of Murphy and Miller if we lower the level of inhibition induced by the modulatory stimulus (decreasing *M* in Fig. 3) or use a feedforward input function that rises rapidly from zero (effectively strengthening the effect of the test stimulus). Thus there is a range of input parameters for which shunting conductance can seem to have a multiplicative effect on neuronal tuning curves. However, we found that, with a stronger modulatory stimulus, the effects of divisive mechanisms of inhibition differ from the effects of subtractive mechanisms.

Our results suggest that it might be possible to determine whether subtractive or divisive mechanisms of inhibition underlie gain modulation by examining the effect of strong suppression on the response curves of neurons. Experimentally, this could be achieved by examining the suppressive effect of high-contrast surround stimuli on V1 neuron responses to lower contrast test stimuli. Our results predict that if a subtractive effect underlies surround suppression, using a high-contrast mask stimulus should result in a subtractive effect on the contrast-response function of the neuron to the test stimulus. If a divisive mechanism underlies surround suppression, however, the effect of the surround stimulus should continue to seem divisive.

Studies have shown that surround suppression is stronger when the surround stimuli are of similar nature (e.g., of the same orientation or spatial frequency) to the test stimulus (Blakemore and Tobin 1972; Cavanaugh et al. 2002b; DeAngelis et.al. 1994; Gilbert and Wiesel 1990; Levitt and Lund 1997; Nelson and Frost 1978). Our model does not reproduce this effect because the modulatory pool is independent of surround parameters other than contrast. However, such an effect could easily be incorporated if modulatory pool input were also tuned for stimulus parameters such as orientation. For example, if the modulatory pool input increases when the surround stimulus is similar to the test stimulus but decreases if the surround stimulus is orthogonally oriented to the test stimulus, the result would be a suppression of neuronal responses to a test stimulus surrounded by a parallel grating but an enhancement of neuronal responses when the test stimulus is surrounded by an orthogonal grating. Because our intent was to focus on the effects of different mechanisms of inhibition, we did not explore reproducing these effects.

Multiplicative scaling of response curves by attention has been reported in multiple studies in visual cortex (McAdams and Maunsell 1999; Treue and Martínez-Trujillo 1999; Williford and Maunsell 2006). In Fig. 6*A*, noisy synaptic activity results in a divisive scaling of the model-tuning curve. For this model to explain the attentional effects observed in vivo, attention should drive a decrease in noisy background input. This is not an implausible situation for cortex, where neurons receive a relatively high level of noisy synaptic input that seems to be independent of external sensory stimuli (Heggelund and Albus 1978; Holt et al. 1996; Schiller et al. 1976; Softky and Koch 1993; Vogels et al. 1989). It should be noted that, because the decrease in noisy input leads to an enhancement of neuronal responses, a decrease in noisy synaptic input to a particular location in cortex will likely lead to an increase in activity as the local neuronal responses are enhanced.

In their study of attention effects on contrast-response functions in V4, Williford and Maunsell (2006) draw a distinction between "activity gain," where total neuronal activity is modulated, and "response gain," where only the activity of the neuron above baseline is modulated. In our model, these two effects are equivalent because the model neuron has negligible baseline activity in the absence of a stimulus.

Other studies (Haenny and Schiller 1988; Martínez-Trujillo and Treue 2004; Spitzer et al. 1988) have reported that attention can cause a narrowing of tuning curves. These effects are more consistent with contrast-gain modulation (Martínez-Trujillo and Treue 2002; Reynolds et al. 2000) than response-gain modulation or activity-gain modulation. In Fig. 6*C*, the narrowing of the tuning curve is accompanied by an enhancement of responses to the preferred stimulus (and likewise a suppression of responses to nonpreferred stimuli). This effect is reminiscent of the feature-based attention effect reported by Martínez-Trujillo and Trueue (2004). In both Fig. 6, *B* and *C*, an increase in modulatory pool activity results in the attended effect.

It has been suggested (Williford and Maunsell 2006) that the task difficulty may be one reason that some studies report response/activity gain modulations, whereas others report a change in contrast gain. It is possible that, as task difficulty increases, local recurrent activity is recruited in a different fashion than for easier tasks. This could lend a circuit-based explanation to the discrepancies between the differing results presented by the various studies.

GRANTS

This research is supported by National Science Foundation Grant IOB-0446129, funds provided by the University of California, and an Alfred P. Sloan Foundation Research Fellowship to F. S. Chance.

REFERENCES

Albrecht DG, Hamilton DB. Striate cortex of monkey and cat: contrast response function. *J Neurophysiol* 48: 217–237, 1982.

Allman J, Miezin F, McGuinness E. Stimulus specific responses from beyond the classical receptive field: neurophysiological mechanisms for local-global comparisons in visual neurons. *Annu Rev Neurosci* 8: 407–430, 1985.

Anderson JS, Lampl I, Gillespie DC, Ferster D. The contribution of noise to contrast invariance of orientation tuning in cat visual cortex. *Science* 290: 1968–1972, 2000.

Anderson JS, Lampl I, Gillespie DC, Ferster D. Membrane potential and conductance changes underlying length tuning of cells in cat primary visual cortex. *J Neurosci* 21: 2104–2112, 2001.

Bernander O, Douglas RJ, Martin KAC, Koch C. Synaptic background activity influences spatiotemporal integration in single pyramidal cells. *Proc Natl Acad Sci* 88: 11569–11573, 1991.

Blakemore C, Tobin EA. Lateral inhibition between orientation detectors in the cat's visual cortex. *Exp Brain Res* 15: 439–440, 1972.

Carandini M, Heeger DJ. Summation and division by neurons in primate visual cortex. *Science* 264: 1333–1336, 1994.

Carandini M, Heeger DJ, Movshon JA. Linearity and normalization in simple cells of the macaque primary visual cortex. *J Neurosci* 17: 8621–8644, 1997.

Cavanaugh JR, Bair W, Movshon JA. Nature and interaction of signals from the receptive field center and surround in macaque V1 neurons. *J Neurophysiol* 88: 2530–2546, 2002a.

Cavanaugh JR, Bair W, Movshon JA. Selectivity and spatial distribution of signals from the receptive field surround in macaque V1 neurons. *J Neurophysiol* 88: 2547–2556, 2002b.

Chance FS, Abbott LF, Reyes AD. Gain modulation from background synaptic input. *Neuron* 35: 773–782, 2002.

Chao-yi L, Creutzfeldt O. The representation of contrast and other stimulus parameters by single neuron in area 17 of the cat. *Pfluegers* 401: 304–314, 1984.

Contreras D, Palmer L. Response to contrast of electrophysiologically defined cell classes in primary visual cortex. *J Neurosci* 23: 6936–6945, 2003.

DeAngelis GC, Freeman RD, Ohzawa I. Length and width tuning of neurons in the cat's primary visual cortex. *J Neurophysiol* 71: 347–374, 1994.

Derrington AM, Lennie P. Spatial and temporal contrast sensitivities of neurons in lateral geniculate nucleus of macaque. *J Physiol* 357: 219–240, 1984.

Destexhe A, Paré D. Impact of network activity on the integrative properties of neocortical pyramidal neurons in vivo. *J Neurophysiol* 81: 1531–1547, 1999.

Doiron B, Longtin A, Berman N, Maler L. Subtractive and divisive inhibition: effect of voltage-dependent inhibitory conductances and noise. *Neural Comput* 13: 227–248, 2001.

Dreher B. Hypercomplex cells in the cat's striate cortex. *Invest Opthalmol* 11: 355–356, 1972.

Fellous JM, Rudolph M, Destexhe A, Sejnowski TJ. Synaptic background noise controls the input/output characteristics of single cells in an in vitro model of in vivo activity. *Neuroscience* 122: 811–829, 2003.

Finn IM, Priebe NJ, Ferster D. The emergence of contrast-invariant orientation tuning in simple cells of cat visual cortex. *Neuron* 54: 137–152, 2007.

Gilbert CD, Wiesel TN. The influence of contextual stimuli on the orientation selectivity of cells in primary visual cortex of the cat. *Vision Res* 30: 1689–1701, 1990.

Haenny PE, Schiller PH. State dependent activity in monkey visual cortex. I. Single cell activity in V1 and V4 on visual tasks. *Exp Brain Res* 69: 225–244, 1988.

Heeger DJ. Normalization of cell responses in cat striate cortex. *Vis Neurosci* 9: 181–197, 1992.

Heeger DJ. Modeling simple cell direction selectivity with normalized, half-squared, linear operators. *J Neurophysiol* 70: 1885–1898, 1993.

Heggelund P, Albus K. Response variability and orientation discrimination of single cells in striate cortex of cat. *Exp Brain Res* 32: 197–211, 1978.

Hirsch JA, Alonso JM, Reid RC, Martinez LM. Synaptic integration in striate cortical simple cells. *J Neurosci* 18: 9517–9528, 1998.

Holt GR, Koch C. Shunting inhibition does not have a divisive effect on firing rates. *Neural Comput* 9: 1001–1013, 1997.

Holt GR, Softky WR, Koch C, Douglas RJ. Comparison of discharge variability in vitro and in vivo in cat visual cortex neurons. *J Neurophysiol* 75: 1806–1814, 1996.

Hubel DH, Wiesel TN. Receptive fields and functional architecture of monkey striate cortex. *J Physiol* 195: 215–243, 1968.

Levitt JB, Lund JS. Contrast dependence of contextual effects in primate visual cortex. *Nature* 387: 73–76, 1997.

Li B, Thompson JK, Duong T, Peterson MR, Freeman RD. Origins of cross-orientation suppression in the visual cortex. *J Neurophysiol* 96: 1755–1764, 2006.

Mariño J, Schummers J, Lyon DC, Schwabe L, Beck O, Wiesing P, Obermayer K, Sur M. Invariant computations in local cortical networks with balanced excitation and inhibition. *Nat Neurosci* 8: 194–201, 2005.

Martínez-Trujillo JC, Treue S. Attentional modulation strength in cortical area MT depends on stimulus contrast. *Neuron* 35: 365–370, 2002.

Martínez-Trujillo JC, Treue S. Feature based attention increases the selectivity of the population responses in primate visual cortex. *Curr Biol* 14: 744–751, 2004.

McAdams CJ, Maunsell JH. Effects of attention on orientation-tuning functions of single neurons in macaque cortical area V4. *J Neurosci* 19: 431–441, 1999.

Mitchell SJ, Silver RA. Shunting inhibition modulates neuronal gain during synaptic excitation. *Neuron* 38: 433–445, 2003.

Monier C, Chavane F, Baudot P, Graham LJ, Frégnac Y. Orientation and direction selectivity of synaptic inputs in visual cortical neurons: a diversity of combinations produces spike tuning. *Neuron* 37: 663–680, 2003.

Murphy BK, Miller KD. Multiplicative gain changes are induced by excitation or inhibition alone. *J Neurosci* 23: 10040–10051, 2003.

Naka KI, Rushton WA. S-potentials from luminosity units in the retina of fish (Cyprinidae). *J Physiol* 185: 587–599, 1966.

Nelson JI, Frost BJ. Orientation-selective inhibition from beyond the classical receptive field. *Brain Res* 139: 359–365, 1978.

Nelson JI, Frost BJ. Intracortical facilitation among co-oriented, coaxially aligned simple cells in cat striate cortex. *Exp Brain Res* 61: 54–61, 1985.

Ozeki H, Sadakane O, Akasaki T, Naito T, Shimegi S, Sato H. Relationship between excitation and inhibition underlying size tuning and contextual response modulation in the cat primary visual cortex. *J Neurosci* 24: 1428–1438, 2004.

Palmer LA, Nafziger JS. Effects of surround motion on receptive-field gain and structure in area 17 of the cat. *Vis Neurosci* 19: 335–353, 2002.

Paré D, Shink E, Gaudreau H, Destexhe A, Lang EJ. Impact of spontaneous synaptic activity on the resting properties of cat neocortical pyramidal neurons in vivo. *J Neurophysiol* 79: 1450–1460, 1998.

Prescott SA, De Koninck Y. Gain control of firing rate by shunting inhibition: roles of synaptic noise and dendritic saturation. *Proc Natl Acad Sci USA* 100: 2076–2081, 2003.

Reynolds JH, Chelazzi L. Attentional modulation of visual processing. *Annu Rev Neurosci* 27: 611–647, 2004.

Reynolds JH, Desimone R. The role of neuronal mechanisms of attention in solving the binding problem. *Neuron* 24: 19–29, 1999.

Reynolds JH, Pasternak T, Desimone R. Attention increases sensitivity of V4 neurons. *Neuron* 26: 703–714, 2000.

Salinas E, Thier P. Gain modulation: a major computation principle of the central nervous system. *Neuron* 27: 15–21, 2000.

Sceniak MP, Hawken MJ, Shapley R. Visual spatial characterization of macaque V1 neurons. *J Neurophysiol* 85: 1873–1887, 2001.

Schiller PH, Finlay BL, Volman SF. Short-term response variability of monkey striate neurons. *Brain Res* 105: 347–349, 1976.

Sclar G, Maunsell JHR, Lennie P. Coding of image contrast in central visual pathways of the macaque monkey. *Vision Res* 30: 1–10, 1990.

Shu Y, Hasenstaub A, Badoual M, Bal T, McCormick DA. Barrages of synaptic activity control the gain and sensitivity of cortical neurons. *J Neurosci* 23: 10388–10401, 2003a.

Shu Y, Hasenstaub A, McCormick DA. Turning on and off recurrent balaced cortical activity. *Nature* 423: 288–293, 2003b.

Sillito AM, Grieve KL, Jones HE, Cuderio J, Davis J. Visual cortical mechanisms detecting focal orientation discontinuities. *Nature* 378: 492–496, 1995.

Softky WR, Koch C. The highly irregular firing of cortical cells is inconsistent with temporal integration of random EPSPs. *J Neurosci* 13: 334–350, 1993.

Spitzer H, Desimone R, Moran J. Increased attention enhances both behavioral and neuronal performances. *Science* 240: 338–340, 1988.

Tolhurst DJ, Dean AF. Evaluation of a linear model of direction selectivity in simple cells of the cat's striate cortex. *Vis Neurosci* 6: 421–428, 1991.

Tolhurst DJ, Heeger DJ. Contrast normalization and a linear model for the directional selectivity of simple cells in cat striate cortex. *Vis Neurosci* 14: 19–25, 1997.

Treue S. Neural correlates of attention in primate visual cortex. *Trends Neurosci* 24: 295–300, 2001.

Treue S, Martínez-Trujillo JC. Feature based attention influences motion processing gain in macaque visual cortex. *Nature* 399: 575–579, 1999.

Ulrich D. Differential arithmetic of shunting inhibition for voltage and spike rate in neocortical pyramidal cells. *Eur J Neurosci* 18: 2159–2165, 2003.

Vogels R, Spileers W, Orban GA. The response variability of striate cortical neurons in the behaving monkey. *Exp Brain Res* 77: 432–436, 1989.

Williford T, Maunsell JH. Effects of spatial attention on contrast response functions in macaque area V4. *J Neurophysiol* 96: 40–54, 2006.